Geochemical Perspectives Letters

© 2023 The Authors
Published by the European Association of Geochemistry

A dual role of methane seepage intensity on calcium isotopic fractionation

J. Wei[1,2,3,4#], T. Wu[1#], X. Miao[5*]

OPEN ACCESS

https://doi.org/10.7185/geochemlet.2303

Abstract

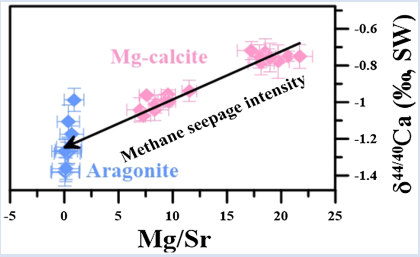

Calcium isotopes are an important indicator to study the global calcium cycle, however the controls on calcium isotopic fractionation in marine carbonates are still under debate. Seep carbonates are widely precipitated on the continental margins. Constraining the calcium isotopic fractionation mechanism operating during the precipitation of seep carbonates is important for understanding the global calcium cycle. In this paper, we report the calcium isotopic composition of authigenic carbonates recovered from seep sites in the South China Sea, and discuss how the methane seepage intensity controls the calcium isotopic fractionation. The result shows that the calcium isotopic composition of the aragonite (−1.17 ‰ SW) is lower than that of the calcite (−0.79 ‰ SW). Compared to calcite, aragonite is usually formed in the near-seafloor environment (or close to the sediment-seawater interface) with a higher precipitation rate, both of which indicate high methane seepage intensity. Therefore, we propose that methane seepage intensity is the fundamental factor in controlling the calcium isotopic fractionation of the seep carbonates. The calcium isotopic composition of the seep carbonates could be used as an important proxy to reconstruct the palaeo cold seep activities and to better constrain the calcium cycling.

Received 3 June 2022 | Accepted 19 December 2022 | Published 23 January 2023

Introduction

Calcium (Ca) is the fifth most abundant element in the Earth's lithosphere and plays an important role in geological and biological processes (Fantle and Tipper, 2014; Griffith and Fantle, 2021). Ca isotopes have been used as a geochemical proxy in the Ca cycle, carbonate (organic and inorganic) mineralisation, and early diagenesis on both global and regional scales (De La Rocha and DePaolo, 2000; Farkaš *et al.*, 2007; Kasemann *et al.*, 2008; Blättler *et al.*, 2021). To ensure the reliability and applicability of this proxy, it is necessary to fully understand the factors affecting Ca isotopic fractionation in the seep carbonates (Gussone *et al.*, 2005; Teichert *et al.*, 2009; Griffith and Fantle, 2021). Experimental and theoretical evidence shows that the precipitated mineral is typically enriched in the lighter isotopes of Ca relative to source fluids, and this relationship is strongly dependent on the precipitation rate (Marriott *et al.*, 2004; Gussone *et al.*, 2005; Blättler *et al.*, 2012, 2021; AlKhatib and Eisenhauer, 2017; Mills *et al.*, 2021).

Cold seep is a widely observed phenomenon on the continental margins (Michaelis *et al.*, 2002; Teichert *et al.*, 2009; Miao *et al.*, 2022), which typically develops extensive authigenic carbonates due to a local increase of alkalinity resulted from sulfate driven anaerobic oxidation of methane (SD-AOM) (Michaelis *et al.*, 2002; Teichert *et al.*, 2009; Blättler *et al.*, 2021). In recent years multiple studies have reported Ca isotope ratios in pore waters and carbonates recovered from methane seeps and discussed the factors controlling the Ca isotopic fractionation in these environments (Teichert *et al.*, 2005; Henderson *et al.*, 2006; Bradbury and Turchyn, 2018; Thiagarajan *et al.*, 2020; Blättler *et al.*, 2021). The impact of the carbonate precipitation rate on the Ca isotopic fractionation has also been demonstrated (Teichert *et al.*, 2005; Henderson *et al.*, 2006; Bradbury and Turchyn, 2018; Thiagarajan *et al.*, 2020; Blättler *et al.*, 2021). However, since the seep carbonate mineral facies and precipitation rate are mainly determined by the methane seepage intensity (Tang *et al.*, 2008; Thiagarajan *et al.*, 2020; Blättler *et al.*, 2021; Smrzka *et al.*, 2021), it is reasonable to anticipate methane seepage intensity is one of the key controls on Ca isotopic fractionation. In addition, the depth of the sulfate-methane transition zone (SMTZ) changes when the methane seepage intensity changes (Blättler *et al.*, 2021). This may affect the extent to which Ca isotope fractionation occurs under shallow open system conditions where dissolved Ca is replenished as carbonate precipitation proceeds, *versus* deeper closed system conditions where there is no replenishment of dissolved Ca during carbonate formation, allowing for the preferential accumulation of ^{44}Ca, which in turn affects the Ca isotopic composition of the carbonates. Therefore, it is believed that methane seepage intensity plays a dual role on the composition of Ca isotopes in the seep carbonates. In this study, we

1. MLR Key Laboratory of Marine Mineral Resources, Guangzhou Marine Geological Survey, Guangzhou 510075, China
2. Southern Marine Science and Engineering Guangdong Laboratory (Guangzhou), Guangzhou 511458, China
3. Sanya Institute of South China Sea Geology, Guangzhou Marine Geological Survey, Sanya 572025, China
4. Academy of South China Sea Geological Science, China Geological Survey, Sanya 572025, China
5. College of Marine Geosciences, Ocean University of China, Key Laboratory of Submarine Geosciences and Prospecting, Qingdao 266100, China
Co-first authors
* Corresponding author (email: xiaomingMr1992@126.com)

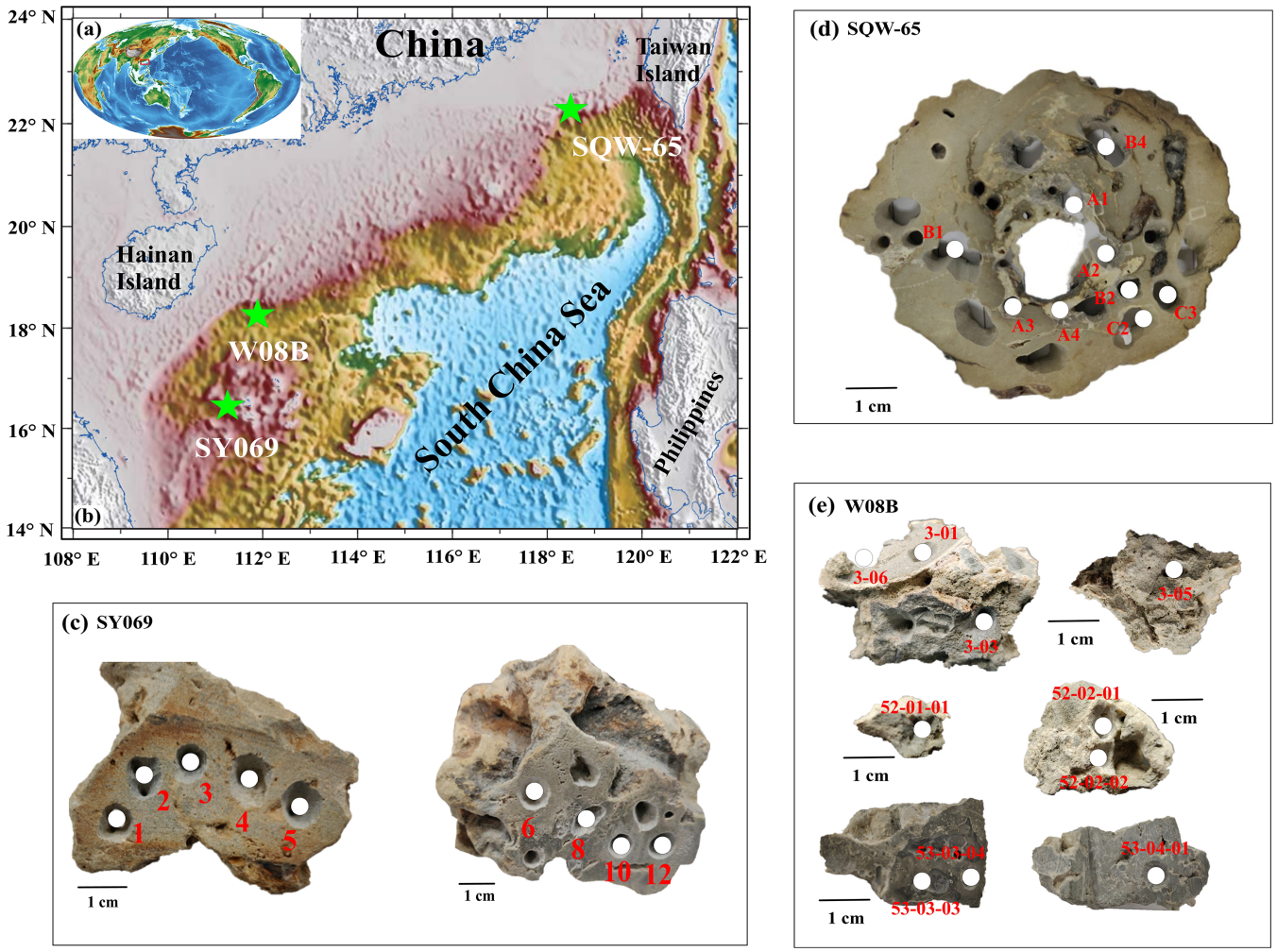

Figure 1 **(a)** World map with the red rectangle showing the study area. **(b)** Topographic map of the study area and the locations of the seep carbonates (green stars). **(c)** SY069 seep carbonate. **(d)** SQW-65 seep carbonate. **(e)** W08B seep carbonate. The sampling locations of the seep carbonates are illustrated by the red dots.

report the mineralogical composition, Ca isotopic composition, major and trace elements of the seep carbonates recovered from different seep sites on the northern continental slope of the South China Sea (Fig. 1), and further discuss the influence of methane seepage intensity on the Ca isotopic fractionation.

Materials and Methods

All the seep carbonates are reported for the first time except W08B (Wei *et al.*, 2020, 2022). The sample location, experimental methods, and data processing are described in the Supporting Information.

Results

The XRD results show that the W08B carbonates are mainly composed of aragonite with a small amount of calcite, while the SY069 and SQW-065 carbonates are dominated by calcite with no aragonite detected. The calcite is primary (Fig. S-2).

The average Sr/Ca and Mg/Ca ratios of W08B are 0.022 and 0.007 ($n = 11$), respectively. The average Sr/Ca and Mg/Ca ratios of SY069 are 0.005 and 0.047 ($n = 9$), respectively. The average Sr/Ca and Mg/Ca ratios of SQW-065 are 0.003 and 0.063 ($n = 10$), respectively (Fig. 2a, Tables S-1, S-2).

Calcium isotopic composition (reported as $\delta^{44/40}$Ca) was determined by a Neptune Plus MC-ICP-MS. The average value of W08B $\delta^{44/40}$Ca is −1.17 ‰ SW ($n = 11$; Fig. 2b,c). The SY069 and SQW-065 $\delta^{44/40}$Ca are relatively high, with average values of −0.92 ‰ SW ($n = 9$) and −0.68 ‰ SW ($n = 10$) (Fig. 2b,c), respectively. The $\delta^{44/40}$Ca of all the samples are negatively correlated with the Sr/Ca ratio ($R^2 = 0.76$) and positively correlated with the Mg/Ca ratio ($R^2 = 0.88$).

Discussion

Precipitation environment of seep carbonates. It is difficult to reconstruct the palaeo carbonate precipitation environment by analysing the pore water because the pore water during carbonate growth cannot be obtained. However, the carbonate mineralogy and geochemistry at methane seeps are mainly influenced by pore water chemistry. Therefore, the seep carbonate precipitation environment can be reconstructed using specific elemental composition and mineral phases (Burton, 1993; Blättler *et al.*, 2021; Smrzka *et al.*, 2021).

Strong methane seepage results in a shallow SMTZ (near the seafloor), the presence of dissolved sulfate is thought to inhibit precipitation of high-Mg carbonates and hence favours aragonite formation (Burton, 1993; Thiagarajan *et al.*, 2020). When the SMTZ is located at deeper sediment horizons (weak

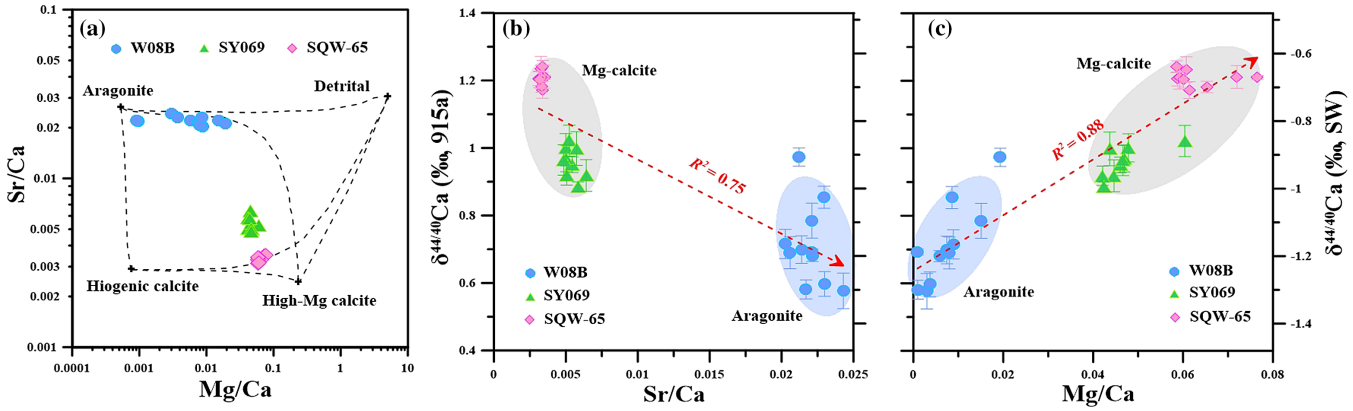

Figure 2 Geochemical properties of the seep carbonates (adapted from Bayon *et al.*, 2007). **(a)** Sr/Ca *vs.* Mg/Ca. **(b)** Sr/Ca *vs.* $\delta^{44/40}$Ca (‰, relative to SRM 915a). **(c)** Mg/Ca ratios *vs.* $\delta^{44/40}$Ca (‰ SW).

methane seepage), high-Mg carbonates generally precipitate (Thiagarajan *et al.*, 2020; Smrzka *et al.*, 2021). In this study, W08B is dominated by aragonite, indicating a shallow SMTZ; while SY069 and SQW-065 are mainly calcite, indicating a deeper SMTZ (Fig. 2a, Table S-1). In addition, studies have shown that the carbonate precipitation rate affects the composition of specific trace element ratios (Sr/Ca, Mg/Ca), and this is the basis for us to potentially use the specific trace element ratios to reconstruct the palaeo carbonate precipitation rate (Luff and Wallmann, 2003; Tang *et al.*, 2008; Thiagarajan *et al.*, 2020; Smrzka *et al.*, 2021). Lab experiments and carbonate diagenesis studies have shown that the partitioning of Mg and Sr, and the fractionation of Ca isotopes in inorganic carbonates are related to the carbonate precipitation rates. For the same fluid composition, high Sr/Ca and low Mg/Ca in the carbonates are associated with high carbonate precipitation rates, while low carbonate precipitation rates result in low Sr/Ca and high Mg/Ca (Luff and Wallmann, 2003; Tang *et al.*, 2008; Thiagarajan *et al.*, 2020; Blättler *et al.*, 2021). In Figure 2a, W08B is dominated by aragonite with high Sr/Ca and low Mg/Ca, indicating a high precipitation rate, while SY069 and SQW-065 are mainly calcite with low Sr/Ca and high Mg/Ca, indicating a low precipitation rate. This is consistent with previous studies, in which the precipitation rate of aragonite is higher than calcite (Luff and Wallmann, 2003; Gussone *et al.*, 2005; Bayon *et al.*, 2007; Thiagarajan *et al.*, 2020; Blättler *et al.*, 2021).

Based on the comprehensive analysis of the mineralogy and geochemistry of carbonates, we conclude that W08B carbonate was formed in a shallow SMTZ with high precipitation rate. However, SY069 and SQW-065 are formed in a deep SMTZ with low precipitation rate. Moreover, it is believed that the main controlling factor of this difference is the methane seepage intensity.

The methane seepage intensity affects the Ca isotopic fractionation. In general, carbonate precipitation results in preferential incorporation of light Ca isotopes, which results in pore waters becoming enriched in heavier Ca isotopes (*i.e.* higher $\delta^{44/40}$Ca values) (Blättler *et al.*, 2012, 2021; AlKhatib and Eisenhauer, 2017; Mills *et al.*, 2021). Lab experiments and theoretical models have shown that the Ca isotopic fractionation of the carbonates increases with higher precipitation rates (Tang *et al.*, 2008; DePaolo, 2011; Nielsen *et al.*, 2012). The $\delta^{44/40}$Ca of these samples showed a negative linear correlation with Sr/Ca ($R^2 = 0.76$; Fig. 2b) and positive linear correlation with Mg/Ca ($R^2 = 0.88$; Fig. 2c). The results indicate that high carbonate precipitation rates (aragonite dominated) lead to the accumulation of light Ca isotopes, while low carbonate precipitation rates (calcite dominated) result in heavy Ca isotopes, which is consistent with current understanding (Gussone *et al.*, 2005; Thiagarajan *et al.*, 2020; Blattler *et al.*, 2021). In normal marine environments, temperature is considered to be a factor controlling the carbonate precipitation rate (Burton and Walter, 1987; Gussone *et al.*, 2005; Thiagarajan *et al.*, 2020). However, based on the *in situ* measurements, the seafloor temperature of W08B (3.5 °C) is similar to that of SY069 (3.1 °C), and slightly lower than that of SQW-065 (8.3 °C) (Supplementary Information). Therefore, temperature difference as the main factor affecting the carbonate precipitation rate can be excluded. In addition, temperature changes in other cold seeps are also not considered as the potential factor in controlling the carbonate precipitation rate (Bradbury and Turchyn, 2018; Thiagarajan *et al.*, 2020; Blattler *et al.*, 2021). However, the HCO_3^- concentration varies significantly because the SD-AOM can generate large amounts of HCO_3^- (Michaelis *et al.*, 2002). Compared with the weak methane seepage, SD-AOM is stronger in the strong methane seepage, and more HCO_3^- will be produced, which increases the alkalinity and the carbonate saturation of the environment (Luff and Wallmann, 2003). In this case, the precipitation rate of the carbonates will be higher in the strong methane seepage than that in the weak methane seepage. Therefore, it is believed that the carbonate precipitation rate caused by the methane seepage intensity is an important factor affecting the Ca isotopic composition.

The seepage intensity not only controls the carbonate precipitation rate, but also controls the depth of the SMTZ (Smrzka *et al.*, 2021), which in turn controls the magnitude of Ca isotopic fractionation. Strong methane seepage results in a shallow SMTZ, and the pore water has a strong mixing effect with the overlying seawater, resulting in a relatively open system (Smrzka *et al.*, 2021). In this scenario, the Ca^{2+} diffusion rate is high, and the ^{40}Ca consumed by the carbonate formation can be replenished from seawater in time, leading to no enrichment in ^{44}Ca. Therefore, light Ca isotopes are more enriched in the aragonite (Fig. 3a). In addition, sufficient SO_4^{2-} supply will also inhibit the formation of calcite by inhibiting Mg entry into the crystal lattice (Burton, 1993; Goetschl *et al.*, 2019), resulting in the precipitation of aragonite, which is consistent with the light Ca isotopic values observed in the W08B aragonite (Fig. 2). Conversely, weak methane seepage results in a deep SMTZ. The thick overlying sediment prevents the exchange of pore water and seawater, resulting in a relatively closed environment (Blattler *et al.*, 2021). The low Ca^{2+} diffusion rate is unable to effectively replenish the consumed ^{40}Ca, therefore, the pore fluid will become enriched in ^{44}Ca, which means later carbonate minerals will also be enriched in ^{44}Ca (Fig. 3b). In addition,

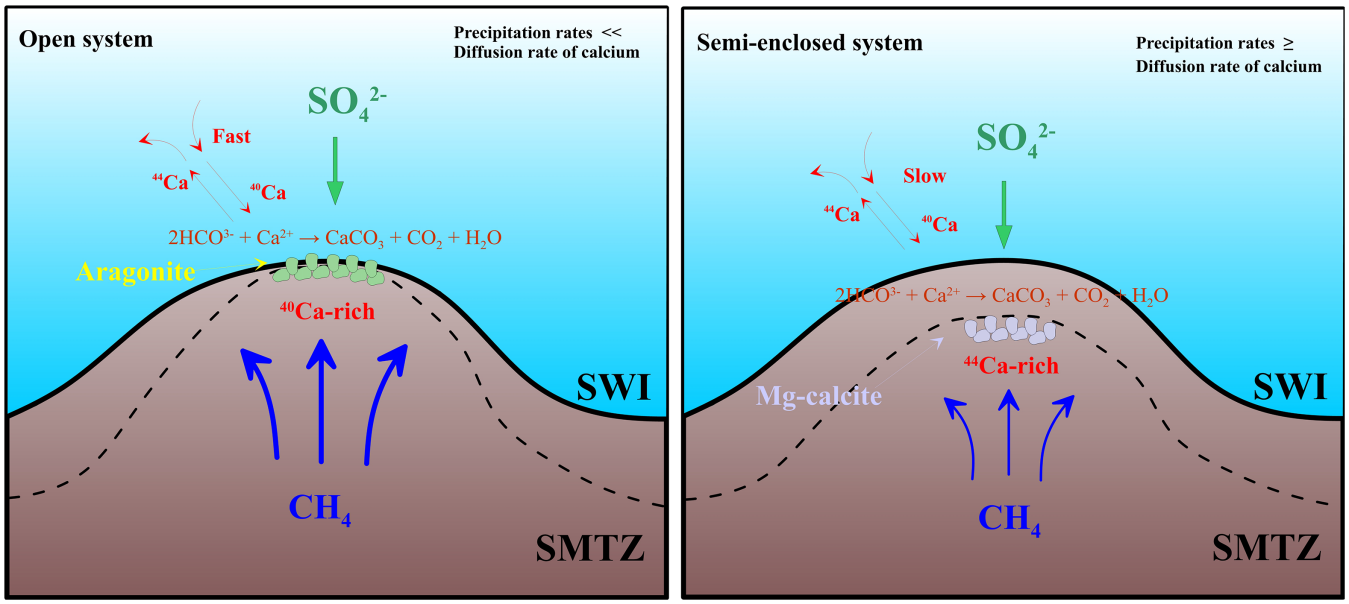

Figure 3 Schematic diagram illustrating the calcium isotopic fractionation in open system *vs.* semi-enclosed system.

carbonate formation in this environment is dominated by calcite (Goetschl *et al.*, 2019; Smrzka *et al.*, 2021), therefore calcite records heavy Ca isotopic values (Fig. 3b). Therefore, it is suggested that methane seepage intensity also controls the openness of the cold seep environment and further affects the Ca isotopic composition.

Conclusions

In the study, a dual role of methane seepage intensity on the Ca isotopic fractionation of the seep carbonates is demonstrated for the first time. It is found that authigenic carbonates collected from different seep sites in the northern continental slope of the South China Sea show obvious differences in Ca isotopes. In the high methane seepage intensity environment, the SMTZ is located in the shallow sediment or even near the seafloor. In a closed system (*i.e.* when the SMTZ is located in the deep sediment), seep carbonate precipitation prefers to incorporate light ^{40}Ca, hence resulting in the enrichment of heavy ^{44}Ca in the pore water. In this case, with time, the ongoing carbonate precipitation (mostly high-Mg calcite) should indeed be accompanied by a heavy Ca isotope composition. In contrast, in an open system (*i.e.* when the SMTZ is located near the seafloor), aragonite is precipitated from a relatively light ^{40}Ca pool in the pore water, hence explaining why the aragonite displays light Ca isotopic composition. These results suggest that the Ca isotope of the seep carbonates is potentially a good proxy for understanding and constraining the palaeo SD-AOM activities in the cold seeps, which is of great significance to study the global calcium cycle.

Acknowledgements

This research was funded by Key Special Project for Introduced Talents Team of Southern Marine Science and Engineering Guangdong Laboratory (Guangzhou) (GML2019ZD0201), National Key Research and Development Program of China (No. 2016YFC0304905-03), Guangdong Province Marine Economic Development (Six Major Marine Industries) Special Fund Project ([2021] No. 58), China Geological Survey Project (No. DD20190224) and Hainan Institute of Chinese Engineering Development Strategies (21-HN-ZT-01). We also thank all the crew and participants in the TS07-02 and TS07-03 expeditions for their support and constructive discussions. JW highly appreciates Mr. Pinxian Wang and Prof Kang Ding for providing the opportunity to participate in the TS07-02 and TS07-03 research cruises. We also appreciate Editor Claudine Stirling and Postdoctoral researcher Tingting Chen (University of Science and Technology of China) for their thoughtful suggestions on a revised draft of the manuscript.

Editor: Claudine Stirling

Additional Information

Supplementary Information accompanies this letter at https://www.geochemicalperspectivesletters.org/article2303.

© 2023 The Authors. This work is distributed under the Creative Commons Attribution Non-Commercial No-Derivatives 4.0 License, which permits unrestricted distribution provided the original author and source are credited. The material may not be adapted (remixed, transformed or built upon) or used for commercial purposes without written permission from the author. Additional information is available at https://www.geochemicalperspectivesletters.org/copyright-and-permissions.

Cite this letter as: Wei, J., Wu, T., Miao, X. (2023) A dual role of methane seepage intensity on calcium isotopic fractionation. *Geochem. Persp. Let.* 24, 38–42. https://doi.org/10.7185/geochemlet.2303

References

AlKhatib, M., Eisenhauer, A. (2017) Calcium and strontium isotope fractionation in aqueous solutions as a function of temperature and reaction rate; I. Calcite. *Geochimica et Cosmochimica Acta* 209, 296–319. https://doi.org/10.1016/j.gca.2016.09.035

Bayon, G., Pierre, C., Etoubleau, J., Voisset, M., Cauquil, E., Marsset, T., Sultan, N., Le Drezen, E., Fouquet, Y. (2007) Sr/Ca and Mg/Ca ratios in Niger Delta

sediments: Implications for authigenic carbonate genesis in cold seep environments. *Marine Geology* 241, 93–109. https://doi.org/10.1016/j.margeo.2007.03.007

Blättler, C.L., Henderson, G.M., Jenkyns, H.C. (2012) Explaining the Phanerozoic Ca isotope history of seawater. *Geology* 40, 843–846. https://doi.org/10.1130/G33191.1

Blättler, C.L., Hong, W.-L., Kirsimäe, K., Higgins, J.A., Lepland, A. (2021) Small calcium isotope fractionation at slow precipitation rates in methane seep authigenic carbonates. *Geochimica et Cosmochimica Acta* 298, 227–239. https://doi.org/10.1016/j.gca.2021.01.001

Bradbury, H.J., Turchyn, A.V. (2018) Calcium isotope fractionation in sedimentary pore fluids from ODP Leg 175: Resolving carbonate recrystallization. *Geochimica et Cosmochimica Acta* 236, 121–139. https://doi.org/10.1016/j.gca.2018.01.040

Burton, E.A. (1993) Controls on marine carbonate cement mineralogy: review and reassessment. *Chemical Geology* 105, 163–179. https://doi.org/10.1016/0009-2541(93)90124-2

Burton, E.A., Walter, L.M. (1987) Relative precipitation rates of aragonite and Mg calcite from seawater: Temperature or carbonate ion control? *Geology* 15, 111–114. https://doi.org/10.1130/0091-7613(1987)15<111:RPROAA>2.0.CO;2

De La Rocha, C.L., DePaolo, D.J. (2000) Isotopic Evidence for Variations in the Marine Calcium Cycle Over the Cenozoic. *Science* 289, 1176–1178. https://doi.org/10.1126/science.289.5482.1176

DePaolo, D.J. (2011) Surface kinetic model for isotopic and trace element fractionation during precipitation of calcite from aqueous solutions. *Geochimica et Cosmochimica Acta* 75, 1039–1056. https://doi.org/10.1016/j.gca.2010.11.020

Fantle, M.S., Tipper, E.T. (2014) Calcium isotopes in the global biogeochemical Ca cycle: Implications for development of a Ca isotope proxy. *Earth-Science Reviews* 129, 148–177. https://doi.org/10.1016/j.earscirev.2013.10.004

Farkaš, J., Böhm, F., Wallmann, K., Blenkinsop, J., Eisenhauer, A., van Geldern, R., Munnecke, A., Voigt, S., Veizer, J. (2007) Calcium isotope record of Phanerozoic oceans: Implications for chemical evolution of seawater and its causative mechanisms. *Geochimica et Cosmochimica Acta* 71, 5117–5134. https://doi.org/10.1016/j.gca.2007.09.004

Goetschl, K.E., Purgstaller, B., Dietzel, M., Mavromatis, V. (2019) Effect of sulfate on magnesium incorporation in low-magnesium calcite. *Geochimica et Cosmochimica Acta* 265, 505–519. https://doi.org/10.1016/j.gca.2019.07.024

Griffith, E., Fantle, M. (2021) *Calcium Isotopes* (Elements in Geochemical Tracers in Earth System Science). Cambridge University Press, Cambridge. https://doi.org/10.1017/9781108853972

Gussone, N., Böhm, F., Eisenhauer, A., Dietzel, M., Heuser, A., Teichert, B.M.A., Reitner, J., Wörheide, G., Dullo, W.-C. (2005) Calcium isotope fractionation in calcite and aragonite. *Geochimica et Cosmochimica Acta* 69, 4485–4494. https://doi.org/10.1016/j.gca.2005.06.003

Henderson, G.M., Chu, N.-C., Bayon, G., Benoit, M. (2006) $\delta^{44/42}$Ca in gas hydrates, porewaters and authigenic carbonates from Niger Delta sediments. *Geochimica et Cosmochimica Acta* 70, A244. https://doi.org/10.1016/j.gca.2006.06.493

Kasemann, S.A., Schmidt, D.N., Pearson, P.N., Hawkesworth, C.J. (2008) Biological and ecological insights into Ca isotopes in planktic foraminifers as a palaeotemperature proxy. *Earth and Planetary Science Letters* 271, 292–302. https://doi.org/10.1016/j.epsl.2008.04.007

Luff, R., Wallmann, K. (2003) Fluid flow, methane fluxes, carbonate precipitation and biogeochemical turnover in gas hydrate-bearing sediments at Hydrate Ridge, Cascadia Margin: numerical modeling and mass balances. *Geochimica et Cosmochimica Acta* 67, 3403–3421. https://doi.org/10.1016/S0016-7037(03)00127-3

Marriott, C.S., Henderson, G.M., Belshaw, N.S., Tudhope, A.W. (2004) Temperature dependence of δ^7Li, δ^{44}Ca and Li/Ca during growth of calcium carbonate. *Earth and Planetary Science Letters* 222, 615–624. https://doi.org/10.1016/j.epsl.2004.02.031

Miao, X., Feng, X., Li, J., Liu, X., Liang, J., Feng, J., Xiao, Q., Dan, X., Wei, J. (2022) Enrichment mechanism of trace elements in pyrite under methane seepage. *Geochemical Perspectives Letters* 21, 18–22. https://doi.org/10.7185/geochemlet.2211

Michaelis, W., Seifert, R., Nauhaus, K., Treude, T., Thiel, V., Blumenberg, M., Knittel, K., Gieseke, A., Peterknecht, K., Pape, T., Boetius, A., Amann, R., Jørgensen, B.B., Widdel, F., Peckmann, J., Pimenov, N.V., Gulin, M.B. (2002) Microbial Reefs in the Black Sea Fueled by Anaerobic Oxidation of Methane. *Science* 297, 1013–1015. https://doi.org/10.1126/science.1072502

Mills, J.V., DePaolo, D.J., Lammers, L.N. (2021) The influence of Ca:CO_3 stoichiometry on Ca isotope fractionation: Implications for process-based models of calcite growth. *Geochimica et Cosmochimica Acta* 298, 87–111. https://doi.org/10.1016/j.gca.2021.01.016

Nielsen, L.C., DePaolo, D.J., De Yoreo, J.J. (2012) Self-consistent ion-by-ion growth model for kinetic isotopic fractionation during calcite precipitation. *Geochimica et Cosmochimica Acta* 86, 166–181. https://doi.org/10.1016/j.gca.2012.02.009

Smrzka, D., Zwicker, J., Lu, Y., Sun, Y., Feng, D., Monien, P., Bohrmann, G., Peckmann, J. (2021) Trace element distribution in methane-seep carbonates: The role of mineralogy and dissolved sulfide. *Chemical Geology* 580, 120357. https://doi.org/10.1016/j.chemgeo.2021.120357

Tang, J., Dietzel, M., Böhm, F., Köhler, S.J., Eisenhauer, A. (2008) Sr^{2+}/Ca^{2+} and $^{44}Ca/^{40}Ca$ fractionation during inorganic calcite formation: II. Ca isotopes. *Geochimica et Cosmochimica Acta* 72, 3733–3745. https://doi.org/10.1016/j.gca.2008.05.033

Teichert, B.M.A., Gussone, N., Eisenhauer, A., Bohrmann, G. (2005) Clathrites: Archives of near-seafloor pore-fluid evolution ($\delta^{44/40}$Ca, δ^{13}C, δ^{18}O) in gas hydrate environments. *Geology* 33, 213–216. https://doi.org/10.1130/G21317.1

Teichert, B.M.A., Gussone, N., Torres, M.E. (2009) Controls on calcium isotope fractionation in sedimentary porewaters. *Earth and Planetary Science Letters* 279, 373–382. https://doi.org/10.1016/j.epsl.2009.01.011

Thiagarajan, N., Crémière, A., Blättler, C., Lepland, A., Kirsimäe, K., Higgins, J., Brunstad, H., Eiler, J. (2020) Stable and clumped isotope characterization of authigenic carbonates in methane cold seep environments. *Geochimica et Cosmochimica Acta* 279, 204–219. https://doi.org/10.1016/j.gca.2020.03.015

Wei, J., Wu, T., Zhang, W., Deng, Y., Xie, R., Feng, J., Liang, J., Lai, P., Zhou, J., Cao, J. (2020) Deeply Buried Authigenic Carbonates in the Qiongdongnan Basin, South China Sea: Implications for Ancient Cold Seep Activities. *Minerals* 10, 1135. https://doi.org/10.3390/min10121135

Wei, J., Wu, T., Miao, X., Su, P. (2022) Massive Natural Gas Hydrate Dissociation During the Penultimate Deglaciation (~130 ka) in the South China Sea. *Frontiers in Marine Science* 9, 875374. https://doi.org/10.3389/fmars.2022.875374

Geochemical Perspectives Letters

© 2023 The Authors
Published by the European Association of Geochemistry

A dual role of methane seepage intensity on calcium isotopic fractionation

J. Wei, T. Wu, X. Miao

Supplementary Information

The Supplementary Information includes:

- Geological Setting and Samples
- Methods
- Tables S-1 to S-4
- Figures S-1 and S-2
- Supplementary Information References

Geological Setting and Samples

The South China Sea is the largest marginal low latitude sea and contains rich reserves of oil and gas. Recently, a comprehensive series of geological and geophysical investigations have shown geophysical evidence and geochemical markers of many methane fluid activities, such as bottom simulating reflectors (BSR), mud volcanoes, mud diapirs, and gas chimneys (Hui *et al*., 2016). Over the years, a group of scientists obtained large amounts of authigenic carbonate from the South China Sea, which proved that long term methane seepage had occurred in this area (Han *et al*., 2008; Tong *et al*., 2013; Liang *et al*., 2017; Feng *et al*., 2018; Wei *et al*., 2022). Therefore, we believe that the South China Sea is an ideal laboratory for the study of methane seepage (Liang *et al*., 2017; Feng *et al*., 2018; Miao *et al*., 2021, 2022).

In 2018, Guangzhou Marine Geological Survey (GMGS) conducted the fifth gas hydrate drilling expedition and drilled at site W08B in the Qiongdongnan Basin. The W08 site was drilled to a depth of ~200 m below the seafloor (mbsf) at 1735 m water depth (Wei *et al*., 2019, 2020, 2022). The bottom water temperature was 3.5 °C. Seep carbonates were discovered at 3 mbsf and 52–54 mbsf (Wei *et al*., 2020, 2022).

In 2018, a joint scientific expedition was conducted using the manned submersible *Shenhaiyongshi* and R/V *Tansuoyihao* from Institute of Deep Sea Science and Engineering. Seep carbonates were recovered from the vicinity of the Ganquan Plateau (SY069 at 1410 m water depth) and Jiulong Methane Reef (SQW-065 at ~500 m water depth) in the South China Sea using the manned submersible *Shenhaiyongshi*. The bottom water temperatures at those sites were 3.1 °C and 8.3 °C, respectively.

Methods

XRD analyses. The analysis and identification of the carbonate mineral composition are performed by X-ray diffraction (Wei *et al*., 2020, 2022). First, the sample was dried (7 hours) and then ground with a mortar. The ground sample was packed into X-ray sample holders for further analysis. The Rigaku SmartLab-9kW X-ray diffractometer was used for sample analysis. For detailed steps, refer to Wei *et al*. (2022).

Stable carbon and oxygen isotopes. The analysis of the stable carbon and oxygen isotopic compositions were performed by using a Thermo MAT-253 isotope ratio mass spectrometer (Wei *et al*., 2022). Supersaturated phosphoric acid was added to the Thermo Kiel IV Carbonate Device unit to extract CO_2 gas. Then, the extracted gas was introduced into the MAT-253 dual inlet system. For detailed steps, refer to Wei *et al*. (2022). And the precisions of $\delta^{13}C$ was ±0.1 ‰, and the precisions of $\delta^{18}O$ was ±0.25 ‰.

Elemental content analyses. Mg, Ca and Sr analyses of samples were conducted on Agiledt 7700e. The sample was dried (7 hours) and then ground with a mortar (200 mesh). Briefly, ~50 mg of sample was weighed out for measuring the Mg, Ca, and Sr content. The sample was then dissolved in 10 mL of 5 vol. % ultra-pure acetic acid, accompanied by agitation in an oscillator (1 hour), with the aim of leaching the carbonate phase. The beaker was then placed in a steel tank and heated at 60 ℃ (24 hours). Subsequently, centrifugation at 4000 rpm for 10 min, the supernatant was filtered with a MillexGP 0.22 μm filter and transferred to a clean PFA beaker. The beaker was placed onto a heating plate to dry the solution at 105 °C. Then, a concentrated mixture of 0.3 mL HNO_3 and 5 mL Milli-Q water was used. The beaker was then placed in a steel tank and heated at 80 ℃ (2 hours). The beaker was placed onto a heating plate to dry the solution at 105 °C. Finally, the solution in beaker was fixed in volume with 2 % nitric acid. Mg, Ca and Sr were measured via ICP-MS. The analytical precision was better than 5 %.

Calcium isotopic analyses. About 50 mg sample powder was used for calcium isotope analyses. Please refer to Lanping *et al*. (2018) and Li *et al*. (2018) for the workflow of sample pre-treatment. And, the calcium isotopes analyses were performed at the Wuhan Sample Solution Analytical Technology Co., Ltd, Hubei, China. The instrument used in this work was a Neptune Plus MC-ICP-MS, produced by Thermo Fisher Scientific of Dreieich, Germany. In addition, calcium isotopic analyses were performed under a "wet" plasma, using a self-lifting micronebuliser injection system with a quartz dual cyclonic-spray chamber and an Savillex 50 μL min^{-1} PFA MicroFlow Teflon nebuliser (Lanping *et al*., 2018; Li *et al*., 2018).

The instrumental drift was corrected by the standard-sample bracketing technique. We report the calcium isotopic composition relative to the reference standard using δ-notation: $\delta^{44/42}Ca_{ref} = [{}^{44}Ca/{}^{42}Ca_{sample}/{}^{44}Ca/{}^{42}Ca_{ref} - 1] \times 1000$ (Li *et al*., 2018). An in-house Alfa Ca standard solution (Lot 9192737) was used as bracketing reference standard in our laboratory (Heuser and Eisenhauer, 2008; Amini *et al*., 2009; Lanping *et al*., 2018; Li *et al*., 2018).

Supplementary Tables

Table S-1 Mineralogical composition of the seep carbonates. LMC, low-magnesium calcite; Dol, dolomite.

Core	Number	Mineral composition (%)				
		LMC	Dol	Aragonite	Quartz	Barite
W08B	3-01	11.1		88.9		
	3-03	13.7		86.3		
	3-05	16.6		77.2	6.1	
	3-06	19.8		71.3	8.9	
	52-01-01	6.6	0.16	93.3		
	52-02-01			100		
	52-02-02			100		
	52-02-04			100		
	53-03-03	9.2		80.7	10.8	
	53-03-04	10.9		81.5	7.5	
	53-04-01	9.5		90.5		
SQW-65	A1	91.1			8.9	
	A2	85.6			14.4	
	A3	81.5			18.5	
	A4	84.6			15.4	
	B1	77			2	
	B2	78			22	
	B4	72.9			27.1	
	C2	52			48	
	C3	55.2			44.8	
	C4	49.4			50.6	
SY069	1	31.9			42.1	26
	2	43			57	
	3	47.7			52.3	
	4	49.3			50.7	
	5	66.6			33.4	
	6	51.3			40.5	6.36
	8	58.9			41.1	
	10	57.1			42.9	
	12	64.2			35.8	

Table S-2 Carbon and oxygen stable isotopic compositions of the seep carbonates.

Core	Number	$\delta^{13}C$ (‰, VPDB)	$\delta^{18}O$ (‰, VPDB)
W08B[a]	3-01	−25.60	3.71
	3-05	−33.77	3.81
	52-02-02	−38.11	4.98
	53-03-04	−38.08	4.57
SQW-65	A1	−42.60	2.25
	A2	−39.13	1.75
	A3	−38.04	1.68
	A4	−42.52	1.74
	B1	−39.62	1.53
	B2	−39.96	1.29
	B4	−41.09	1.96
	C2	−33.97	0.63
	C3	−33.77	0.65
	C4	−33.20	0.30
SY069	1	−34.24	1.36
	2	−35.7	3.73
	3	−41.3	3.28
	4	−39.78	3.04
	5	−41.45	3.6
	6	−43.45	3.29
	8	−39.63	3.59
	10	−41.19	3.71
	12	−40.74	3.61

[a] Data from Wei *et al*. (2020).

Table S-3 Major and trace element compositions of the seep carbonates.

Core	Number	Mg (μg/g)	Ca (μg/g)	Sr (μg/g)	Mg/Ca	Sr/Ca
W08B	3-01	2668	299866	6075	0.009	0.020
	3-03	1984	339376	7513	0.006	0.022
	3-05	2488	333309	7130	0.007	0.021
	3-06	2492	311398	6413	0.008	0.021
	52-01-01	2789	325330	7470	0.009	0.023
	52-02-01	4555	301668	6670	0.015	0.022
	52-02-02	6641	343345	7284	0.019	0.021
	52-02-04	1033	344670	8373	0.003	0.024
	53-03-03	378	389851	8462	0.001	0.022
	53-03-04	360	391181	8653	0.001	0.022
	53-04-01	1277	344764	7926	0.004	0.023
SQW-65	A1	19035	264397	922	0.0720	0.0035
	A2	16872	220398	777	0.0766	0.0035
	A3	14495	236081	799	0.0614	0.0034
	A4	16574	253657	841	0.0653	0.0033
	B1	12765	210231	689	0.0607	0.0033
	B2	12475	212191	663	0.0588	0.0031
	B4	13724	228298	723	0.0601	0.0032
	C2	9879	166713	549	0.0593	0.0033
	C3	9002	153695	521	0.0586	0.0034
	C4	10191	176050	578	0.0579	0.0033
SY069	1	5087	113926	730	0.0446	0.0064
	2	6971	165516	837	0.0421	0.0051
	3	9884	214762	1171	0.0460	0.0055
	4	8864	209191	1224	0.0424	0.0059
	5	10554	220499	1101	0.0479	0.0050
	6	8047	133231	699	0.0604	0.0052
	8	10131	231955	1334	0.0437	0.0058
	10	10809	230348	1160	0.0469	0.0050
	12	10431	223635	1087	0.0466	0.0049

Table S-4 Calcium isotopic compositions of the seep carbonates.

Core	Number	$\delta^{44/42}Ca_{SRM\ 915a}$ (‰)	2 s.d.	$\delta^{43/42}Ca_{SRM\ 915a}$ (‰)	2 s.d.	$\delta^{44/40}Ca_{SRM\ 915a}$ (‰)	$\delta^{44/40}Ca_{SW}$ (‰)
W08B	3-01	0.35	0.04	0.14	0.09	0.72	−1.16
	3-03	0.33	0.02	0.16	0.10	0.68	−1.20
	3-05	0.34	0.04	0.17	0.04	0.70	−1.18
	3-06	0.34	0.05	0.14	0.08	0.69	−1.19
	52-01-01	0.28	0.05	0.11	0.08	0.58	−1.30
	52-02-01	0.28	0.03	0.14	0.07	0.58	−1.30
	52-02-02	0.34	0.01	0.17	0.03	0.69	−1.19
	52-02-04	0.29	0.04	0.12	0.05	0.60	−1.28
	53-03-03	0.42	0.03	0.21	0.03	0.85	−1.03
	53-03-04	0.38	0.05	0.20	0.06	0.78	−1.10
	53-04-01	0.48	0.03	0.22	0.01	0.97	−0.91
SQW-65	A1	0.59	0.03	0.29	0.03	1.21	−0.67
	A2	0.59	0.01	0.26	0.07	1.21	−0.67
	A3	0.57	0.02	0.26	0.06	1.17	−0.71
	A4	0.58	0.02	0.28	0.09	1.18	−0.70
	B1	0.60	0.04	0.31	0.07	1.23	−0.65
	B2	0.59	0.02	0.26	0.05	1.21	−0.67
	B4	0.59	0.02	0.28	0.08	1.20	−0.68
	C2	0.59	0.04	0.30	0.06	1.21	−0.67
	C3	0.61	0.02	0.27	0.05	1.24	−0.64
	C4	0.57	0.05	0.29	0.07	1.17	−0.71
SY069	1	0.45	0.05	0.19	0.07	0.92	−0.96
	2	0.45	0.03	0.20	0.06	0.92	−0.96
	3	0.46	0.02	0.21	0.05	0.95	−0.93
	4	0.43	0.01	0.20	0.03	0.89	−0.99
	5	0.49	0.04	0.21	0.03	1.00	−0.88
	6	0.50	0.05	0.23	0.06	1.02	−0.86
	8	0.49	0.05	0.23	0.01	1.00	−0.88
	10	0.47	0.04	0.24	0.04	0.97	−0.91
	12	0.47	0.05	0.24	0.02	0.96	−0.92

Supplementary Figures

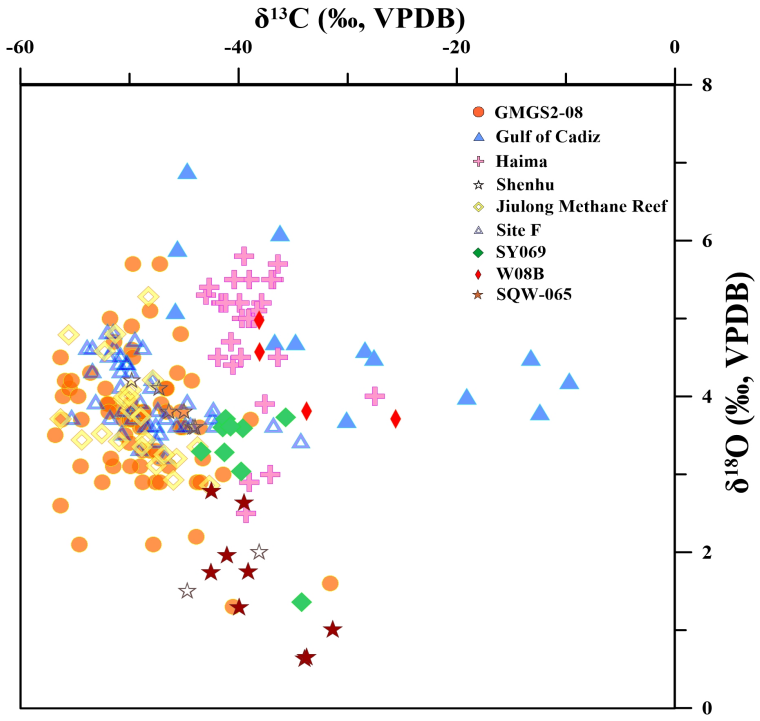

Figure S-1 Carbon and oxygen isotopic compositions of the seep carbonates: GMGS2-08 (Deng *et al*., 2021), Gulf of Cadiz (Wang *et al*., 2015), Haima (Liang *et al*., 2017), Shenhu (Tong *et al*., 2013), Jiulong Methane Reef (Han *et al*., 2008), Site F (Feng and Chen, 2015), SY069 (this study), W08B (Wei *et al*., 2020, 2022), and SQW-065 (this study).

Carbon isotopic compositions of the seep carbonates are an important proxy to identify the source of the carbonate formation (Bayon *et al*., 2013, 2015; Feng *et al*., 2018; Wei *et al*., 2020; Deng *et al*., 2021). It has been known that the $\delta^{13}C$ value in methane is very low (around −110 ‰ to −30 ‰; Sackett, 1978; Whiticar, 1999). In the process of cold seep activity, the $\delta^{13}C$ poor methane is transferred to the seep carbonates by SD-AOM, which results in obvious carbon isotopic composition difference between cold seep carbonate and normal marine carbonate (Peckmann *et al*., 2001; Peckmann and Thiel, 2004). As shown in Figure S-1, the carbon isotopic composition of the carbonate in the seep sites of this study is between −43.45 ‰ and −25.60 ‰, which is very similar to those of the Gulf of Cadiz, Haima seep, Jiulong Methane Reef, Site F and other cold seep carbonates in the world (Han *et al*., 2008; Tong *et al*., 2013; Feng and Chen, 2015; Wang *et al*., 2015; Liang *et al*., 2017; Deng *et al*., 2021). In addition, the carbon isotope of the cold seep carbonate is usually higher than that of methane as influenced by different processes of seawater, organic matter, and residual carbon sources in the methane producing zones (Paull *et al*., 1992). Therefore, it is believed that the carbon of the carbonates is mainly from methane.

Here, the $\delta^{18}O$ value of the authigenic carbonates is high (Fig. S-1), which is very similar to other cold seep carbonates (Han *et al*., 2008; Tong *et al*., 2013; Feng and Chen, 2015; Wang *et al*., 2015; Liang *et al*., 2017; Deng *et al*., 2021) and is thought to be caused by ^{18}O-rich fluid from gas hydrate dissociation (Chen *et al*., 2019; Deng *et al*., 2021; Wei *et al*., 2020, 2022). Although, it is shown that dehydration of clay minerals in deep sediments also produces ^{18}O-rich fluids (Hesse, 2003), given the widespread presence of hydrates in the South China Sea (Chen *et al*., 2019; Wei *et al*., 2019), we believe that clay dehydration may not be the main cause of ^{18}O-rich fluids. Therefore, it is proposed that ^{18}O-rich fluid is mainly from gas hydrate dissociation.

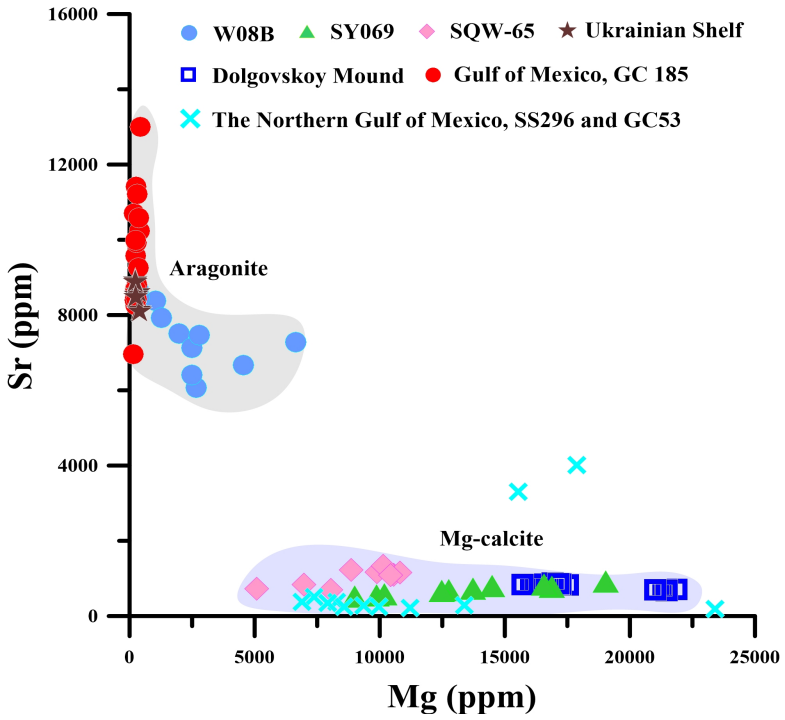

Figure S-2 Magnesium and strontium content of the seep carbonates: W08B (this study), SY069 (this study), SQW-065 (this study), Ukrainian Shelf (Smrzka *et al*., 2021), Dolgovskoy Mound (Smrzka *et al*., 2021), Gulf of Mexico GC185 (Smrzka *et al*., 2021) and The Northern Gulf of Mexico (SS296 and GC53; Huang *et al*., 2020).

Aragonite and calcite are the two main types of carbonates. By comparing the Mg and Sr contents of these two carbonates, it is shown that aragonite has a higher Sr and a lower Mg, while calcite is just the opposite (Huang *et al*., 2020; Smrzka *et al*., 2021). In Figure S-2, W08B showed obvious aragonite characteristics, SY069 and SQW-65 showed typical calcite characteristics. However, aragonite is considered to be a metastable phase, which is prone to recrystallise into low-Mg during burial diagenesis (Al-aasm and Veizer, 1986; Burton, 1993). Therefore, in order to ensure that the calcite records the original environmental information, we need to explore whether the calcite is primary or secondary. It is shown that calcite formed from aragonite recrystallisation has higher Sr content (Brand and Veizer, 1980; Denison *et al*., 1994; Himmler *et al*., 2011; Swart, 2015). However, this phenomenon was not found in SY069 and SQW-65. Therefore, we believe that SY069 and SQW-65 belong to primary calcite.

Supplementary Information References

Al-Aasm, I.S., Veizer, J. (1986) Diagenetic stabilization of aragonite and low-Mg calcite; II, Stable isotopes in rudists. *Journal of Sedimentary Research* 56, 763–770. https://doi.org/10.2110/jsr.56.763

Amini, M., Eisenhauer, A., Böhm, F., Holmden, C., Kreissig, K., Hauff, F., Jochum, K.P. (2009) Calcium Isotopes ($\delta^{44/40}$Ca) in MPI-DING Reference Glasses, USGS Rock Powders and Various Rocks: Evidence for Ca Isotope Fractionation in Terrestrial Silicates. *Geostandards and Geoanalytical Research* 33, 231–247. https://doi.org/10.1111/j.1751-908X.2009.00903.x

Bayon, G., Dupré, S., Ponzevera, E., Etoubleau, J., Chéron, S., Pierre, C., Mascle, J., Boetius, A., de Lange, G.J. (2013) Formation of carbonate chimneys in the Mediterranean Sea linked to deep-water oxygen depletion. *Nature Geoscience* 6, 755–760. https://doi.org/10.1038/ngeo1888

Bayon, G., Henderson, G.M., Etoubleau, J., Caprais, J.-C., Ruffine, L., Marsset, T., Dennielou, B., Cauquil, E., Voisset, M., Sultan, N. (2015) U-Th isotope constraints on gas hydrate and pockmark dynamics at the Niger delta margin. *Marine Geology* 370, 87–98. https://doi.org/10.1016/j.margeo.2015.10.012

Brand, U., Veizer, J. (1980) Chemical diagenesis of a multicomponent carbonate system; 1, Trace elements. *Journal of Sedimentary Research* 50, 1219–1236. https://doi.org/10.1306/212F7BB7-2B24-11D7-8648000102C1865D

Burton, E.A. (1993) Controls on marine carbonate cement mineralogy: review and reassessment. *Chemical Geology* 105, 163–179. https://doi.org/10.1016/0009-2541(93)90124-2

Chen, F., Wang, X., Li, N., Cao, J., Bayon, G., Peckmann, J., Hu, Y., Gong, S., Cheng, H., Edwards, R.L., Ning, Y., Jin, M., Huang, H., Wu, C., Sun, Y., Chen, H., Zhou, Y., Chen, D., Feng, D. (2019) Gas Hydrate Dissociation During Sea-Level Highstand Inferred From U/Th Dating of Seep Carbonate From the South China Sea. *Geophysical Research Letters* 46, 13928–13938. https://doi.org/10.1029/2019GL085643

Deng, Y., Chen, F., Guo, Q., Hu, Y., Chen, D., Yang, S., Cao, J., Chen, H., Wei, R., Cheng, S., Zhou, J., Liu, C., Jiang, X., Zhu, J. (2021) Possible Links Between Methane Seepages and Glacial-Interglacial Transitions in the South China Sea. *Geophysical Research Letters* 48, e2020GL091429. https://doi.org/10.1029/2020GL091429

Denison, R.E., Koepnick, R.B., Fletcher, A., Howell, M.W., Callaway, W.S. (1994) Criteria for the retention of original seawater $^{87}Sr/^{86}Sr$ in ancient shelf limestones. *Chemical Geology* 112, 131–143. https://doi.org/10.1016/0009-2541(94)90110-4

Feng, D., Chen, D. (2015) Authigenic carbonates from an active cold seep of the northern South China Sea: New insights into fluid sources and past seepage activity. *Deep Sea Research Part II: Topical Studies in Oceanography* 122, 74–83. https://doi.org/10.1016/j.dsr2.2015.02.003

Feng, D., Qiu, J.-W., Hu, Y., Peckmann, J., Guan, H., Tong, H., Chen, C., Chen, J., Gong, S., Li, N., Chen, D. (2018) Cold seep systems in the South China Sea: An overview. *Journal of Asian Earth Sciences* 168, 3–16. https://doi.org/10.1016/j.jseaes.2018.09.021

Han, X., Suess, E., Huang, Y., Wu, N., Bohrmann, G., Su, X., Eisenhauer, A., Rehder, G., Fang, Y. (2008) Jiulong methane reef: Microbial mediation of seep carbonates in the South China Sea. *Marine Geology* 249, 243–256. https://doi.org/10.1016/j.margeo.2007.11.012

Hesse, R. (2003) Pore water anomalies of submarine gas-hydrate zones as tool to assess hydrate abundance and distribution in the subsurface: What have we learned in the past decade? *Earth-Science Reviews* 61, 149–179. https://doi.org/10.1016/S0012-8252(02)00117-4

Heuser, A., Eisenhauer, A. (2008) The Calcium Isotope Composition ($\delta^{44/40}$Ca) of NIST SRM 915b and NIST SRM 1486. *Geostandards and Geoanalytical Research* 32, 311–315. https://doi.org/10.1111/j.1751-908X.2008.00877.x

Himmler, T., Brinkmann, F., Bohrmann, G., Peckmann, J. (2011) Corrosion patterns of seep-carbonates from the eastern Mediterranean Sea. *Terra Nova* 23, 206–212. https://doi.org/10.1111/j.1365-3121.2011.01000.x

Huang, H., Wang, X., Gong, S., Krake, N., Jin, M., Li, N., Birgel, D., Peckmann, J., Cheng, M., Roberts, H.H., Chen, D., Feng, D. (2020) New constraints on the formation of hydrocarbon-derived low magnesium calcite at brine seeps in the Gulf of Mexico. *Sedimentary Geology* 398, 105572. https://doi.org/10.1016/j.sedgeo.2019.105572

Hui, G., Li, S., Guo, L., Zhang, G., Gong, Y., Somerville, I.D., Zhang, Y., Zheng, Q., Zang, Y. (2016) Source and accumulation of gas hydrate in the northern margin of the South China Sea. *Marine and Petroleum Geology* 69, 127–145. https://doi.org/10.1016/j.marpetgeo.2015.10.009

Lanping, F., Zhou, L., Yang, L., Zhang, W., Wang, Q., Shuoyun, T., Hu, Z. (2018). A rapid and simple single-stage method for Ca separation from geological and biological samples for isotopic analysis by MC-ICP-MS. *Journal of Analytical Atomic Spectrometry* 33, 413–421. https://doi.org/10.1039/C7JA00370F

Liang, Q., Hu, Y., Feng, D., Peckmann, J., Chen, L., Yang, S., Liang, J., Tao, J., Chen, D. (2017) Authigenic carbonates from newly discovered active cold seeps on the northwestern slope of the South China Sea: Constraints on fluid sources, formation environments, and seepage dynamics. *Deep Sea Research Part I: Oceanographic Research Papers* 124, 31–41. https://doi.org/10.1016/j.dsr.2017.04.015

Li, M., Lei, Y., Feng, L., Wang, Z., Belshaw, N.S., Hu, Z., Liu, Y., Zhou, L., Chen, H., Chai, X. (2018) High-precision Ca isotopic measurement using a large geometry high resolution MC-ICP-MS with a dummy bucket. *Journal of Analytical Atomic Spectrometry* 33, 1707–1719. https://doi.org/10.1039/C8JA00234G

Miao, X., Feng, X., Liu, X., Li, J., Wei, J. (2021) Effects of methane seepage activity on the morphology and geochemistry of authigenic pyrite. *Marine and Petroleum Geology* 133, 105231. https://doi.org/10.1016/j.marpetgeo.2021.105231

Miao, X., Feng, X., Li, J., Liu, X., Liang, J., Feng, J., Xiao, Q., Dan, X., Wei, J. (2022) Enrichment mechanism of trace elements in pyrite under methane seepage. *Geochemical Perspectives Letters* 21, 18–22. https://doi.org/10.7185/geochemlet.2211

Paull, C.K., Chanton, J.P., Neumann, A.C., Coston, J.A., Martens, C.S., Showers, W. (1992) Indicators of methane-derived carbonates and chemosynthetic organic carbon deposits: examples from the Florida Escarpment. *Palaios* 7, 361–375. https://doi.org/10.2307/3514822

Peckmann, J., Thiel, V. (2004) Carbon cycling at ancient methane–seeps. *Chemical Geology* 205, 443–467. https://doi.org/10.1016/j.chemgeo.2003.12.025

Peckmann, J., Reimer, A., Luth, U., Luth, C., Hansen, B.T., Heinicke, C., Hoefs, J., Reitner, J. (2001) Methane-derived carbonates and authigenic pyrite from the northwestern Black Sea. *Marine Geology* 177, 129–150. https://doi.org/10.1016/S0025-3227(01)00128-1

Sackett, W.M. (1978) Carbon and hydrogen isotope effects during the thermocatalytic production of hydrocarbons in laboratory simulation experiments. *Geochimica et Cosmochimica Acta* 42, 571–580. https://doi.org/10.1016/0016-7037(78)90002-9

Smrzka, D., Zwicker, J., Lu, Y., Sun, Y., Feng, D., Monien, P., Bohrmann, G., Peckmann, J. (2021) Trace element distribution in methane-seep carbonates: The role of mineralogy and dissolved sulfide. *Chemical Geology* 580, 120357. https://doi.org/10.1016/j.chemgeo.2021.120357

Swart, P.K. (2015) The geochemistry of carbonate diagenesis: The past, present and future. *Sedimentology* 62, 1233–1304. https://doi.org/10.1111/sed.12205

Tong, H., Feng, D., Cheng, H., Yang, S., Wang, H., Min, A.G., Edwards, R.L., Chen, Z., Chen, D. (2013) Authigenic carbonates from seeps on the northern continental slope of the South China Sea: New insights into fluid sources and geochronology. *Marine and Petroleum Geology* 43, 260–271. https://doi.org/10.1016/j.marpetgeo.2013.01.011

Wang, S., Magalhães, V.H., Pinheiro, L.M., Liu, J., Yan, W. (2015) Tracing the composition, fluid source and formation conditions of the methane-derived authigenic carbonates in the Gulf of Cadiz with rare earth elements and stable isotopes. *Marine and Petroleum Geology* 68, 192–205. https://doi.org/10.1016/j.marpetgeo.2015.08.022

Wei, J., Liang, J., Lu, J., Zhang, W., He, Y. (2019) Characteristics and dynamics of gas hydrate systems in the northwestern South China Sea - Results of the fifth gas hydrate drilling expedition. *Marine and Petroleum Geology* 110, 287–298. https://doi.org/10.1016/j.marpetgeo.2019.07.028

Wei, J., Wu, T., Zhang, W., Deng, Y., Xie, R., Feng, J., Liang, J., Lai, P., Zhou, J., Cao, J. (2020) Deeply Buried Authigenic Carbonates in the Qiongdongnan Basin, South China Sea: Implications for Ancient Cold Seep Activities. *Minerals* 10, 1135. https://doi.org/10.3390/min10121135

Wei, J., Wu, T., Miao, X., Su, P. (2022) Massive Natural Gas Hydrate Dissociation During the Penultimate Deglaciation (~130 ka) in the South China Sea. *Frontiers in Marine Science* 9, 875374. https://doi.org/10.3389/fmars.2022.875374

Whiticar, M.J. (1999) Carbon and hydrogen isotope systematics of bacterial formation and oxidation of methane. *Chemical Geology* 161, 291–314. https://doi.org/10.1016/S0009-2541(99)00092-3